Integrative Biology

Accepted Manuscript

ROYAL SOCIETY OF CHEMISTRY

www.rsc.org/ibiology

Tissue-Culture Light Sheet Fluorescence Microscopy (TC-LSFM) allows long-term imaging of three-dimensional cell cultures under controlled conditions

Francesco Pampaloni[1#*], Ulrich Berge[2,4,#] , Anastasios Marmaras[2,], Peter Horvath[3],

Ruth Kroschewski[2*], Ernst H.K. Stelzer[1]

[1]*Buchmann Institute for Molecular Life Sciences (BMLS)*

Institute for Cell Biology and Neurosciences (FB15, IZN)

Goethe Universität Frankfurt am Main

Max-von-Laue-Str. 15, D-60438 Frankfurt am Main, Germany

[2]*ETH Zürich, Institute of Biochemistry, Otto-Stern-Weg 3, CH-8093 Zürich, Switzerland*

[3]*ETH Zürich, Light Microscopy Centre, Otto-Stern-Weg 3, CH-8093 Zürich, Switzerland*

[4]*Life Science Zurich Graduate School, Molecular Life Science PhD program*

[#] Contributed equally

*Corresponding authors:

Francesco Pampaloni, email: Francesco.pampaloni@physikalischebiologie.de

Ruth Kroschewski, email: Ruth.Kroschewski@bc.biol.ethz.ch

Insight box

Conventional fluorescence microscopes have limitations to image live gel-embedded three-dimensional cell cultures. These limitations are the high light absorption and scattering in thick specimens, photobleaching, phototoxicity, as well as a short penetration depth. We have overcome these limitations with a light sheet-based fluorescence microscope (LSFM) optimized for three-dimensional cell cultures, dubbed "tissue culture-LSFM" (TC-LSFM). We achieved three-dimensional live imaging of MDCK cell aggregate formation for up to five days within a millimeter-sized gel. The TC-LSFM exhibits low phototoxicity as shown by the low frequency of cell death events during the whole imaging time. The TC-LSFM and the

specimen preparation presented here can be universally applied to gel-embedded cell systems. Thus, the TC-LSFM represents a first-choice technique for the investigation three-dimensional cell cultures.

Abstract

Fluorescence long-term imaging of cellular processes in three-dimensional cultures requires the control of media supply, temperature, and pH, as well as minimal photodamage. We describe a system based on a light sheet fluorescence microscope (LSFM), which is optimized for long-term, multi-position imaging of three-dimensional in-gel cell cultures. The system integrates a stable culture condition control system in the optical path of the light-sheet microscope. A further essential element is a biocompatible agarose container suitable for the LSFM, in which any cell type can be cultured in different gel matrices. The TC-LSFM allows studying any *in vitro* cultured cell type reacting to, dividing in, or migrating through a three-dimensional extracellular matrix (ECM) gel. For this reason we dubbed it "tissue culture-LSFM" (TC-LSFM). The TC-LSFM system allows fast imaging at multiple locations within a millimeter-sized ECM gel. This increases the number of analyzed events and allows testing population effects. As an example, we show the maturation of a cyst of MDCK (canine kidney epithelial) cells over a period of three days. Moreover, we imaged, tracked, and analyzed MDCK cells during the first five days of cell aggregate formation and discovered a remarkable heterogeneity in cell cycle lengths and an interesting cell death pattern. Thus, TC-LSFM allows performing new long-term assays assessing cellular behavior in three-dimensional ECM-gel cultures. For example migration, invasion or differentiation in epithelial cell systems, stem cells, as well as cancer cells can be investigated.

Introduction

Long-term live fluorescence imaging is a powerful method to observe time-dependent processes in single cells, tissues, as well as in smaller entire multicellular organisms [1], and is essential in developmental[2], stem cell[3, 4], as well as cancer cell biology[5]. Yet photo-bleaching and phototoxicity in illuminated specimen, as well as the constancy of the specimen's environmental parameters (e.g. temperature, pH, nutrients, and oxygenation) still represent challenges in long-term experiments with living cells[1].

In vitro 3D-tissue culture systems are meso-scale model systems (more than one cell, yet less than a full multicellular organism) to study how cells form multicellular ensembles. Cells in such cultures phenotypically recapitulate early stages of organ formation[6-8]. Specifically, 3D-

tissue culture allows studying how single mammalian cells from established cell lines or primary cultures, which are fully embedded in soft matrices, form and organize themselves into multi-cellular aggregates. These systems provide a controllable physiological environmental context, yet less complex than whole organisms as drosophila, zebrafish, or mice. Typical examples are the MDCK canine kidney epithelial cell line and the MCF-10a human breast epithelial cells, which form 3D structures reaching in about 7 days dimensions of 500 x 500 x 500 μm^3 and consisting of about 500 cells[9, 10].

To ensure constant culture conditions during the several day-long imaging period of such *in vitro* 3D-tissue cultures, the cells have to be constantly supplied with fresh culture medium. Thus, feeding new nutrients and also removing accumulating metabolites allows preservation of the start culture condition. Also, the initial physiological pH, oxygenation, and temperature should be maintained for the entire duration of the experiment. An additional challenge in long-term three-dimensional fluorescence microscopy is any light-induced specimen perturbation. The fluorescence illumination produces oxygen radicals in the specimen, which induce oxidative stress rapidly perturbing the cells' physiologic reaction that shall be studied in the first place[11]. Also, oxygen radicals cause rapid photobleaching of the fluorophores limiting thus the observation window. A high recording speed in three dimensions is a further key issue, especially if switching to shorter imaging intervals during a long-term experiment is required, e.g. in order to capture rapid changes occurring during mitosis. Clearly, the higher the recording speed the lower are the phototoxic effects. Additionally, it is desirable to image the events of interest at multiple locations in a specimen to increase the number of analyzed events in case of quantitative analyses or to assess positional effects within the ECM gel. In fact, ECM remodeling over time might affect the entire cell population in the imaged culture sample[12].

The issues of phototoxicity, photobleaching, high recording speed and three-dimensional imaging have been improved by employing a spinning-disk confocal microscope[13], a highly optimized wide-field multi-mode, super-resolution microscope (such as the Optical Microscope eXperimental - OMX)[14], and a light sheet-based fluorescence microscope (LSFM)[15, 16]. Among these three microscopes, the LSFM is particularly gentle towards living samples. With the light-sheet microscope, the specimen is irradiated with an extremely low energy of 1.7 µJ at 488 nm in the illumination plane[17, 18]. This is at least two orders of magnitude less than the energy required by confocal microscope in the focal plane[17]. Besides these outstanding properties, the LSFM provides true optical sectioning[16], which represents a significant improvement over deconvolved wide-field imaging as performed in previous

works[19]. With LSFM, long-term fluorescence imaging of developing zebrafish, *Danio Rerio*, and drosophila embryos for up to 67 hours have been performed without impairing embryonic development[16, 17, 20]. The LSFM has also been proposed as the microscope of choice for the imaging of three-dimensional cell cultures[21-23]. Imaging of live MDCK cysts and tumor cell spheroids at selected time points have been successfully performed with a LSFM employing high numerical aperture water-dipping objective lenses[24].

Recently, a LSFM has been used for time-lapse imaging of live cellular spheroids in phytagel containers over a time of roughly 100 minutes[13]. Here, we went a step further and present a set-up, the TC-LSFM (**Figure 1**, **Figure 2**), that allowed during controlled culture conditions truly long-term, as over several days, three-dimensional imaging of MDCK cells tagged with fluorescent reporter molecules and embedded in collagen matrix.

Material and methods

Cell culture

Low-passage MDCK type II cells stably expressing GFP-tagged F-actin (GFP-actin) (a gift from Gabriel Fenteany, University of Illinois) were employed for long-term recording of the MDCK cyst growth. MDCK II cells transfected with a plasmid encoding YFP-tagged histone2B (H2B-YFP)[25] were used for the lineage studies. Transfection was performed with Effectene (Qiagen, Valencia, CA, USA) and FACS sorted. In tests, collagen-embedded live wild-type MDCK II were stained with 5 µM of the red-fluorescent cytoplasmic and nuclear stain Syto61 (Invitrogen, S-11343) for 30 min. All the employed MDCK cells were maintained in 1000 mg/ml glucose Dulbecco's modified Eagle's medium (DMEM, D2902 Sigma-Aldrich) supplemented with 2.2 g/l of sodium bicarbonate, 10% fetal bovine serum (FBS), 100 IU/ml penicillin, and 100 mg/ml streptomycin. The culture medium of both GFP-actin and H2B-YFP cells contained in addition 0.6 mg/ml G418 (Invitrogen, Carlsbad, CA, USA). The cells were cultured at 37 °C and 5% CO2 in a humidified cell culture incubator before seeding them for experiments in collagen.

Agarose container

In order to provide an optically clear and biocompatible container for the soft three-dimensional collagen gel, we employed in the TC-LSFM-perfusion chamber (**Figure 1**, **Figure 2**) a specimen holder made of agarose (**Supplementary Figures 1-4**). The used agarose gel is mechanically stable and does not impair the diffusion of oxygen and nutrients to the cells. The container has an inner diameter of ~1.5 mm, an outer diameter of ~3 mm, a

length of ~15 mm, and a total inner volume of ~25 µl. These dimensions have been chosen as the best compromise between mechanical stability, wall thickness, and pipetting ease. We produce conical-bottom agarose containers (**Supplementary Figure 4**) by employing a custom made stainless-steel template, consisting of stainless-steel tube and stainless-steel plunger (**Supplementary Figure 1**). Working at room temperature, the template is immersed in a 2 ml tube filled with 1% high-melting point agarose. The agarose is sucked into the template by pulling the plunger. The filled template is then cooled to 4°C for 5 minutes to quickly harden the agarose gel. Once the agarose is hardened, the plunger is removed from the template. The agarose container is easily separated from the template by completely immersing the container in PBS and by gently grabbing it from the top with a sharp-tip precision forceps (**Supplementary Figure 4a-d**). The containers can be stored for several weeks at 4°C in PBS with 1% penicillin or streptomycin.

Preparation of the cell-gel mixture

At 80% confluence in a tissue culture plate single cell suspensions are made using 0.05% trypsin or EDTA. The cells are washed with supplemented DMEM, and re-suspended in the same medium to a final density of $4 \cdot 10^5$ cells/ml. DMEM medium 1× (Sigma-Aldrich D2902, supplemented with 2.2 g/l $NaHCO_3$ and 10% FCS), $NaHCO_3/Na_2CO_3$ buffer (pH 9, 7.5 g/100 ml H_2O each), DMEM 10× (prepared from Sigma D2902), and bovine type I hydrated collagen (Koken AteloCell I AC-30, 3.0 mg/ml, Japan) are mixed on ice at a 1:5.5:6.5:50 volume ratio. The final collagen concentration of 1.2 mg/ml is obtained by mixing the collagen solution with the cell suspension in DMEM at a 1:1 ratio. Incubation for 10-15 minutes at 37°C induces the gelation of the cell-collagen mixture.

Cell seeding in the agarose container

A precision stainless steel forceps with sharp angled tips is well suited for the gentle manipulation of the agarose containers. An agarose container is placed vertically against the inner wall of a petri dish (as shown in **Supplementary Figure 4d**). The container is completely emptied from the storage PBS with a 1 ml syringe connected to a 0.55×25 mm needle (24 G × 1''). Then, the MDCK cells suspended in collagen gel are seeded in the agarose container by using a 1 ml-syringe with a hypodermic needle of small gauge (e.g. a 0.55×25 mm needle, 24 G × 1''). No air bubble should form in the cell suspension during injection. Next, the container is placed in the cell incubator at 37°C and 5% CO_2 and the collagen is allowed to polymerize for 15 minutes. Finally, the container is connected with the

custom made connector for the LSFM (**Supplementary Figure 2**) and is ready to be inserted into the TC-LSFM perfusion chamber (**Figure 1, Supplementary Figure 4e-f**).

LSFM perfusion chamber

The perfusion chamber has a volume of about 15 ml. Perfusion is required because the CO_2 diffusion into the media through the air/liquid interphase is too slow for the large volume of medium contained in the chamber. The material of the chamber is polyoxymethylene (POM), a chemically inert, autoclavable and biocompatible plastic (**Supplementary Figure 4e-f**). The chamber heating element is realized by sandwiching a heating foil between two 2 mm thick aluminum plates. The heating element is firmly screwed to the chamber bottom, which is 1 mm thin to ensure efficient heat transmission. The temperature inside the chamber is measured by a PT-100 sensor, inserted in the chamber's wall and positioned at the same level of the specimen. The sensor's output is fed into a custom-built Proportional-Integral-Derivative (PID) control circuit (EMBL Heidelberg, Electronic Workshop), which maintains a constant media temperature (**Supplementary Figure 5**). The inlet and outlet of the perfusion chamber are connected to the media supply bottle and to the media waste bottle, respectively, as shown in **Figure 2**). More detailed technical information on the heating system are given in the document **Supplementary technical information 1**. The document **Supplementary technical information 2** illustrates the procedure employed to measure the temperature distribution in the TC-LSFM chamber.

Set up of the gas exchange system

The gas exchange system allows 1) to efficiently equilibrate the perfused media with CO_2, 2) to oxygenate the media and 3) to maintain a constant pH in the perfusion chamber for the duration of the experiment. The media supply tubing is composed of a gas-impermeable rubber tubing (Reichelt Chemietechnik, Germany, EPDM/PP pharmaceutical tubing, 1.6 mm internal diameter, 4.8 mm external diameter), connected to a 4 m-long gas-permeable thin silicon tubing (Reichelt Chemietechnik, Germany, 1 mm internal diameter, 2 mm external diameter). The silicon tube spirals around a cylindrical support and is inserted into a Plexiglas container where a CO_2/air mixture (typically 5% CO_2/air) is continuously flown by a gas controller (Pecon GmbH, Germany) (**Figure 2**, **Supplementary Figure 6**). The CO_2/air mixture diffuses through the thin silicon tube and saturates the perfused media. With a 5% CO_2/air mixture the media, supplemented with 3.11 g/l $NaHCO_3$, rapidly reaches a pH=7.4 (**Supplementary Figure 6**). The supply tubing is pre-filled with media before connecting it to the inlet. This is done by sucking the media into the tube with a Pasteur pipette connected

to the vacuum line. Pre-filling avoids air bubbles in the chamber once the peristaltic pump is started. The waste media tubing is connected to the outlet. Both media supply and waste tubes are folded into a two-way peristaltic pump (Ismatec REGLO), which regulates the inlet and outlet flows. The flow speed employed in the experiment was the slowest possible for the pump, i.e. ~300µl/min, which replaces the entire 15 ml inside the specimen chamber once every 50 min.

Imaging

The LSFM employed in this work has been described elsewhere[26]. Briefly, the sample is illuminated by a laser light sheet (**Figure 1**). An array of lasers provides the wavelengths (typically 405 nm, 488 nm, 543 nm, 633 nm) required for the excitation of several fluorophores. A cylindrical lens is used to focus a collimated laser beam along one dimension, thereby creating a single plane of light in the excitation path. Since cylindrical lenses with the required NA are usually not sufficiently corrected for optical aberrations, an objective lens (e.g., CZ Epiplan 10 /0.2, or CZ Plan-Neofluar 5x/0.16, Carl Zeiss AG, Germany) is employed in combination with the cylindrical lens[26]. The use of objective lenses allows to obtain a diffraction-limited laser light sheet with a thickness of about 2 µm.

The resulting fluorescence emitted from the illuminated plane of the specimen is collected with a camera placed in an optical system that is arranged perpendicularly to the optical axis of the light sheet. Standard parts used in conventional fluorescence microscope are employed for the detection, i.e. an objective lens, a filter wheel, and a tube lens (**Figure 1a**). The sample is moved along the detection axis (i.e. perpendicular to the plane of the light sheet) with a typical step size of 1 µm and a three-dimensional data stack is recorded. The emission signal from the illuminated plane is collected by a Carl Zeiss water dipping N-Achroplan 40x 0.8 NA objective lens and a Hamamatsu Orca HR camera. A custom made acquisition software controls all the LSFM functions. The main functions include the recording of z-stacks and time-lapses of z-stacks, as well as the recording of a sequence of multiple locations pre-selected in the entire specimen volume.

Data processing

The processing of the raw images recorded during MDCK aggregate growth (rendering and segmentation) was performed with ImageJ (Wayne Rasband, http://rsbweb.nih.gov/ij/), Amira (VSG, Burlington, MA, USA) and Imaris 7.1.1 (Bitplane, Schlieren, Switzerland). The raw images were stacked in the xy-, xz-, and yz-planes for each position and time point employing a custom made Matlab code. Each three-dimensional stack comprised up to 120 single xy-

frames. The slice spacing (i.e. axial pitch) in the stack was Δz=1 µm. Transmitted light images were recorded every other time point. The individual stacks were loaded in Imaris and the nuclei were automatically segmented using its "surface generation function" by applying the "local-contrast background subtraction" function and the "individually adjusted threshold" function. Tracking of the nuclei was performed automatically by auto-regression motion, setting a maximal distance of 10 µm and a maximal gap size of 0. The automated segmentation and tracking results were corrected and critical aspects verified by two independent researchers. Cell IDs and links were exported using a custom made Imaris Xtension script written in Matlab. All following calculations were also performed in Matlab. Briefly, cell lineage trees were generated with nodes representing cell division events and edges representing the cells' interphase time, if a mitosis followed. Cell cycle length was defined as the time between the first appearance of two discrete fluorescent chromosomal regions and the time point before the next start of mitosis. Cell cycle lengths were univocally assigned to the respective cell IDs. Cells that had undergone the same number of completed mitoses belong to the same generation G*x*. Generation 1 (G1) refers to the founder cell of an aggregate. All statistical tests on the data were performed in Matlab. If not otherwise mentioned, the Kruskal-Wallis test was used to test the significance of the differences between medians.

Results and discussion

Long-term imaging of MDCK aggregates expressing fluorescent reporter proteins is required to decipher individual steps involved in the *in vitro* formation of cysts (a cyst is defined as a monolayer of cells enclosing a light microscopically resolvable central lumen). To accomplish this goal, the TC-LSFM was developed and validated. First, in order to test whether confining the cell-collagen gel mixture in an agarose container impairs MDCK cyst formation, MDCK cells were seeded in the agarose containers (as described in the materials and methods section) for seven days at 37°C and 5% CO_2 in a conventional tissue culture incubator. Morphologically normal MDCK cysts, also observed in a parallel collagen gel culture in a petri dish, developed in the container seven days after seeding single cells in the matrix (**Supplementary Figure 3**). Thus, we conclude that confinement in the agarose container does not impair cyst formation. Next, we verified that the agarose container itself does not induce imaging artifacts in the LSFM images. One container with collagen-embedded MDCK cells was incubated for 30 minutes with the fluorescent dye Syto61, which highlights both the nuclei and the cytoplasm, and subsequently washed with PBS and

mounted in the TC-LSFM for imaging. Three-dimensional z-stacks of the embedded live aggregates were recorded at a depth of about 300 µm inside the container. **Figure 3** shows that the cellular organization of the aggregates could be resolved in three dimensions and that they appear qualitatively similar to MDCK aggregates grown outside agarose containers (see e.g.[24, 27]). **Supplementary Figure 8a** shows one MDCK cyst embedded in collagen and imaged outside the agarose container with an epi-fluorescence microscope. **Supplementary Figure 8b** shows one MDCK cysts embedded in collagen and imaged within the agarose container with the TC-LSFM. By visually comparing the two images, it is apparent that the presence of the agarose container does not impair the imaging quality. Thus, confining collagen-embedded MDCK cells in the agarose containers neither impairs cyst development nor introduces significant aberrations in LSFM images.

As phototoxicity is an enormous obstacle in long-term three-dimensional fluorescent imaging of large live specimens, we tested for it in two experimental conditions. First, the ability of the TC-LSFM to support MDCK cell proliferation and lumen enlargement during time-lapse imaging over several days was assessed. A representative small aggregate of four MDCK cells was selected within an agarose container and imaged with the TC-LSFM for 72 hours at intervals of two hours. At each time point a three-dimensional image stack of 50 single xy frames spaced 0.5 µm along the z-axis was recorded. The combined increase in cell number and lumen volume that leads to a net increase of the cyst size are observable in the images recorded with the TC-LSFM (**Figure 4**). Remarkably, no cell death was detectable in that time window. The observed cyst development follows a pattern that is consistent with what is reported for MDCK cell aggregates observed with the phase contrast microscope, but clearly delivers more measurable details[28]. **The Supplementary Movie 1** show the development of the MDCK aggregate recorded with the TC-LSFM in both the phase contrast and the fluorescence channels. Under this experimental condition no sign of phototoxicity was detectable here and in further similar aggregates (data not shown). Due to the high quality of the images and the optical sectioning ability of the TC-LSFM, the isosurface rendering of the fluorescence images was possible giving access to the total cyst volume and the volume of the internal lumen, which are basic parameters required for the quantitative study of cyst development (**Supplementary Figure 7)**.

In our second test, we recorded the divisions of several single cells and two-cell MDCK aggregates expressing YFP-tagged histone2B in two distinct experiments, tracked their division-based relationships and determined the corresponding cell cycle lengths and cell death events during aggregate formation. Low-passage H2B-YFP expressing MDCK cells

seeded in collagen were imaged at multiple positions with the TC-LSFM up to a maximum recording time of 126 hours (i.e. five days) in two channels (YFP-fluorescence and bright field), with a recording interval of two hours. In total, the formations of 12 small three-dimensional aggregates were recorded and analyzed (**Figure 5**). The association of single cells with a pre-existing aggregate was never observed during the time-lapse imaging. This shows that each recorded cell aggregate is the result of cell division only. In all the 12 developments only once 2 nuclei segregate away from the main group of 9 nuclei (at t = 78 hours, a late imaging time point) (**Figure 6**). Phase contrast reveals that these 2 cells stayed in contact with the main aggregate (**Supplementary Movie 2**). Thus, we never observed a complete cell dissociation occurring from any imaged aggregate. To be able to analyze the division-based relationships between the cells, which does not include their spatial relationships, cell lineage trees of all imaged aggregates were generated with a Matlab routine as described in the method section. For that goal, cell divisions were identified in the fluorescent images by the appearance of a pair of nuclei whose morphology and position is compatible with telophase (e.g. **Figure 6a**, arrowhead at t = 52 hours). The cells are highly motile during the formation of an aggregate (**Figure 6b** and **Supplementary Movie 3**), but the three-dimensional imaging allows the tracking of individual cells at each time point. We determined a cell cycle length only if the microscope captured the generation and the following division of a given cell. Thus, in the aggregate shown in **Figure 6** two cell cycle lengths of G2 cells, four cell cycle lengths of G3 cells and 3 cell cycle lengths of G4 cells could be obtained.

Seven aggregates were recorded in a first experiment (E1), and five in a second experiment (E2) (**Figure 5a**). The analysis of all twelve lineage trees reveals that the median cell cycle length is 24 hours. Remarkably, the median cell cycle lengths of individual trees differed significantly ($p=0.0002$), yet the median cell cycle lengths between the experiments E1 and E2 were not significantly different ($p=0.1$) (**Figure 5a**). This suggests that the results from different three-dimensional cell cultures are comparable, but that in the individual trees a high cell cycle length variability is present. We assessed at which time point the cell cycle lengths started to diverge during the formation of an aggregate by analyzing the dependence of the cell cycle length on the number of generations. We found that neither median cell cycle lengths nor variances of cell cycle lengths per generation changed significantly over the generations in all aggregates (Kruskal-Wallis, $p=0.3$, Levene's test, $p=0.3$, respectively, **Figure 5b**). Thus, a strong intrinsic heterogeneity of cell cycle length persists over all recorded generations indicating that laser-induced effects, e.g. phototoxicity, do not bias the

variability of cell cycle lengths between daughter cells and thus of the lineage trees. We found that even two daughter cells often differed in their cell cycle lengths. Specifically, the cell cycle lengths of two daughter cells differed in 20% of the cases (7/36 cases) by one or more than one entire cell cycle length if compared to the cell cycle of the slower of the two daughter cells. In one extreme case, the cell cycle duration of two daughter cells at generation 6 differed in such a comparison even by a factor of 2.5. However, another observed sibling pair in generation 6 did not differ that strongly. These results suggest that the variability in cell cycle length is neither dependent on the lineage tree nor on the generation (**Figure 7**). Future investigations will determine whether cell cycle length variability depends on the position of the cell in the aggregate.

To assess the influence of phototoxicity more directly, we monitored nuclear fragmentation (**Figure 8a**, arrowhead). This allowed us to quantify the number of cell death events over time. In case phototoxicity was due to laser illumination, cell death events should increase with the imaging time. However, this was not the case as shown in **Figure 8b** ($p = 0.41$ from a robust linear regression), demonstrating that phototoxicity does not detectably influence the formation of MDCK aggregate. Remarkably, if cell death events occurred they occurred multiple times within one lineage, namely in 7 out of the 12 lineages (58%). And even more strikingly, in a total of 29 cell deaths that occurred in these seven lineage trees, 26 of them were in daughter cells (90%), suggesting that certain lineages or sub-lineages might be more prone to cell death than others. This remarkable biological indication is worth being corroborated in future studies similarly to[29]. In summary, the constant cell death frequency over the imaging time and the constant heterogeneity of cell cycle lengths over generations strongly suggest that the TC-LSFM system provides a sufficiently stable growth and imaging environment for several days.

Summary and perspective

A TC-LSFM consists of a light sheet-based fluorescence microscope combined with a biocompatible sample holder, a perfusion chamber, in which the cells are cultured, and a culture environment control system; all optimized for the optical path of the LSFM. The integration of these elements and the combination with the intrinsic low phototoxicity of the LSFM is the innovation that allowed us to image over several days collagen-embedded fluorescently tagged MDCK cells in three dimensions, in the absence of detectable phototoxicity. Indeed, cell death events were very low or even absent in many of the developments during the imaging period.

Thus, the TC-LSFM will allow investigating a plethora of different experimental conditions in the future. In this work, we have achieved the imaging of the development of single collagen-embedded MDCK cells to aggregates composed of up to 12 cells. The high quality of the data allowed us the subsequent data analysis and revealed a high heterogeneity of cell cycle duration and a remarkable cell death pattern, both of which are worth to be analyzed in more detail in the future. These experimental results were only possible due to several technical advances implemented in the TC-LSFM. First, we integrated a culture environment control, composed by a perfusion system with a peristaltic pump, temperature control, and a gas exchanger system to the optical configuration of a LSFM. An LSFM-chamber with temperature and gas control has been previously published by Lorenzo et al.[13]. In the system of Lorenzo et al., an incubator box surrounds the LSFM-chamber. The temperature and the CO_2 concentration are controlled within the box. The pH and oxygenation of the medium in the chamber are expected to be regulated by the diffusion of the CO_2/air mixture flushed at the air/liquid interface. A commercially available LSFM (Zeiss Lightsheet Z.1) features a chamber with a Peltier-based temperature control. Similarly to the system presented in Lorenzo et al., a controlled CO_2/air atmosphere is flushed at the air-liquid interphase in the chamber. The main drawback of both systems is that the large volume of the medium in the chamber prevents an efficient diffusion of the gas down to the specimen's depth. In fact, it has been shown that several hours are required in order to equilibrate a changing O_2/air mixture with the medium contained in conventional tissue culture plates[30]. In conventional tissue culture lab-ware the surface-to-volume ratio of the medium is usually much larger than in a typical LSFM chamber. Thus, it is likely that a reliable control of the medium pH and oxygenation is not possible in both system. In contrast, we demonstrated by using a long and thin silicon tube as gas exchanger that the pH of the medium can be efficiently varied within few minutes. Therefore, the TC-LSFM implementation is in our opinion very well suited to perform experiments in which the pH and/or oxygenation need to be precisely controlled for long-term imaging, hypoxia, and hyperoxia experiments. In addition, only with this system drug perfusion can be intimately linked to culture condition controls. The existing systems, such the one of Lorenzo et al., or the commercial LSFM can be easily adapted to the TC-LSFM implementation.

Next, we elaborated a special gel mounting protocol, employing transparent and bio-compatible agarose containers that do not interfere with the imaging and the physiology of the cells. This system allows experiments that cannot be achieved with conventional live-cell microscopes, such as epifluorescence and confocal microscopes. Both confocal and

epifluorescence microscopes illuminate the whole specimen during recording inducing thus strong photobleaching everywhere in the specimen. Moreover, confocal and also spinning disk confocal microscopes have a slow recording speed, which further increases phototoxicity and photobleaching.

Previous studies analyzing fluorescently tagged MDCK cells in collagen with epifluorescence microscope combined with deconvolution identified the stages leading to MDCK cysts. However, in these experiments the live imaging was performed only over a few hours (6 hours) and the aggregates consisted maximally of 2 or 3 cells[19, 31]. However, when larger three-dimensional specimens, such as aggregates consisting of tens of mammalian cells, are imaged with a wide-field fluorescence microscope and deconvolved, that method will result in blurry images with low signal-to-noise ratio that are difficult to segment and to further analyze. Phototoxicity is also a serious issue in wide-field imaging of fluorescently-tagged cells and limits its application to a few hours. In contrast, with the TC-LSFM even large MDCK aggregates could be truly optically sectioned and thus segmented. Taken together, the TC-LSFM allows the recording of dynamic processes of fluorescently tagged MDCK cells in three dimensions over a period of days, with an excellent spatio-temporal resolution, a very good signal-to-noise ratio and parallel recording of multiple locations in the sample, and all of this in absence of sign of photobleaching. To our knowledge, this is the first time that three-dimensional fluorescence time-lapse imaging of MDCK aggregates over days was reported. We would like to point out that both the cell type and the matrix, as well as the medium supplements can be changed depending on the specific scientific question, thus dramatically widening the range of applications. Indeed, the perfusion system allows for the administration of a medium-soluble drug at specific times during an experiment and its removal without interfering with the cell culture. This ensures precision and reversibility. Thus, besides continuous also transient effects of growth factors, ion concentrations, pharmacologically test drugs can now be tested for during the assembly of such meso-scale multicellular structures.

Further outstanding features of the TC-LSFM system are the possibility of fast imaging and a large choice of objectives from low to high magnification and numerical aperture. This allows for a great experimental flexibility. For instance, during a long-term experiment with long intervals (hours) it is possible to switch to very short intervals (few minutes) to record highly dynamic events. Thus, not only cellular self-assembly processes, as shown in this work, can be analyzed, but also cancer cell migration studies are possible, where e.g. the highly motile leading edges could be followed. Since high-numerical aperture objectives can

be employed, also sub-cellular structures such as actin microfilaments, microtubules, or organelles can be investigated during extended periods of time.

In summary, we demonstrated long-term (several days) live three-dimensional imaging of collagen-embedded fluorescently-tagged mammalian cells with the TC-LSFM in the absence of detectable phototoxic effects. The way is now paved to perform diverse controlled and perturbed long-term studies with all sorts of cell types embedded in three-dimensional matrices, investigating quantitatively and in parallel the mechanisms of e.g. cell polarization, cancer cohort migration, and cellular self-assembly.

Authors contribution

FP developed the TC-LSFM chamber, the perfusion system, the agarose container method, performed experiments on growing cysts, processed the data, and wrote the manuscript. UB performed the experiments on MDCK clonal aggregates, wrote Matlab scripts and processed the data. AM wrote a Matlab code for image processing. PH wrote a Matlab code allowing lineage tree analysis. EHKS contributed to the design of the system and the experiments. RK initiated and supervised the work on MDCK clonal aggregates and wrote the manuscript. All authors read and revised the manuscript.

Acknowledgements

We thank for the financial support of the Swiss National Science Foundation (SNSF 3100-061596.00/1) to RK, the EMBO short-term fellowship (ASTF 95-2009) to UB. FP and EHKS thank the Deutsche Forschungsgemeinschaft (DFG) and the Cluster of Excellence Frankfurt for Macromolecular Complexes (CEF-MC) for the financial support. FP and EHKS thank Georg Ritter (Electronic Workshop, EMBL) and Leo Burger (Mechanical Workshop, EMBL).

The authors declare that they have no conflict of interest.

References

1. P. G. Gritsenko, O. Ilina and P. Friedl, The Journal of pathology, 2012, 226, 185-199.
2. P. A. Gagliardi, L. di Blasio, F. Orso, G. Seano, R. Sessa, D. Taverna, F. Bussolino and L. Primo, Neoplasia, 2012, 14, 719-731.
3. M. Roccio, D. Schmitter, M. Knobloch, Y. Okawa, D. Sage and M. P. Lutolf, Development, 2013, 140, 459-470.
4. M. A. Lancaster, M. Renner, C. A. Martin, D. Wenzel, L. S. Bicknell, M. E. Hurles, T. Homfray, J. M. Penninger, A. P. Jackson and J. A. Knoblich, Nature, 2013, 501, 373-379.
5. P. Friedl and K. Wolf, Nat Rev Cancer, 2003, 3, 362-374.

6. J. J. Campbell, L. A. Botos, T. J. Sargeant, N. Davidenko, R. E. Cameron and C. J. Watson, Integrative biology : quantitative biosciences from nano to macro, 2014.
7. M. M. Zegers, Seminars in cell & developmental biology, 2014.
8. B. M. Baker and C. S. Chen, Journal of cell science, 2012, 125, 3015-3024.
9. A. L. Pollack, R. B. Runyan and K. E. Mostov, Developmental biology, 1998, 204, 64-79.
10. J. Debnath, K. R. Mills, N. L. Collins, M. J. Reginato, S. K. Muthuswamy and J. S. Brugge, Cell, 2002, 111, 29-40.
11. V. Nikoletopoulou and N. Tavernarakis, Biotechnol J, 2012, 7, 1156-1168.
12. A. Marmaras, U. Berge, A. Ferrari, V. Kurtcuoglu, D. Poulikakos and R. Kroschewski, Cytoskeleton (Hoboken), 2010, 67, 224-240.
13. C. Lorenzo, C. Frongia, R. Jorand, J. Fehrenbach, P. Weiss, A. Maandhui, G. Gay, B. Ducommun and V. Lobjois, Cell Div, 2011, 6, 22.
14. I. M. Dobbie, E. King, R. M. Parton, P. M. Carlton, J. W. Sedat, J. R. Swedlow and I. Davis, Cold Spring Harbor protocols, 2011, 2011, 899-909.
15. J. Huisken and D. Y. Stainier, Development, 2009, 136, 1963-1975.
16. J. Huisken, J. Swoger, F. Del Bene, J. Wittbrodt and E. H. Stelzer, Science, 2004, 305, 1007-1009.
17. P. J. Keller, A. D. Schmidt, J. Wittbrodt and E. H. Stelzer, Science, 2008, 322, 1065-1069.
18. P. J. Keller and E. H. Stelzer, Curr Opin Neurobiol, 2008, 18, 624-632.
19. A. Ferrari, A. Veligodskiy, U. Berge, M. S. Lucas and R. Kroschewski, Journal of cell science, 2008, 121, 3649-3663.
20. P. J. Keller, A. D. Schmidt, A. Santella, K. Khairy, Z. Bao, J. Wittbrodt and E. H. Stelzer, Nat Methods, 2010, 7, 637-642.
21. F. Pampaloni, N. Ansari and E. H. Stelzer, Cell and tissue research, 2013, 352, 161-177.
22. F. Pampaloni, E. G. Reynaud and E. H. Stelzer, Nat Rev Mol Cell Biol, 2007, 8, 839-845.
23. F. Pampaloni, E. H. Stelzer and A. Masotti, Recent Pat Biotechnol, 2009, 3, 103-117.
24. P. J. Verveer, J. Swoger, F. Pampaloni, K. Greger, M. Marcello and E. H. Stelzer, Nat Methods, 2007, 4, 311-313.
25. D. Gerlich, J. Beaudouin, B. Kalbfuss, N. Daigle, R. Eils and J. Ellenberg, Cell, 2003, 112, 751-764.
26. K. Greger, J. Swoger and E. H. Stelzer, The Review of scientific instruments, 2007, 78, 023705.
27. J. Swoger, F. Pampaloni and E. H. Stelzer, Cold Spring Harbor protocols, 2014, 2014.
28. W. Yu, X. Fang, A. Ewald, K. Wong, C. A. Hunt, Z. Werb, M. A. Matthay and K. Mostov, Molecular biology of the cell, 2007, 18, 1693-1700.
29. S. L. Spencer, S. Gaudet, J. G. Albeck, J. M. Burke and P. K. Sorger, Nature, 2009, 459, 428-432.
30. C. B. Allen, B. K. Schneider and C. W. White, American journal of physiology. Lung cellular and molecular physiology, 2001, 281, L1021-1027.
31. D. Zeng, A. Ferrari, J. Ulmer, A. Veligodskiy, P. Fischer, J. Spatz, Y. Ventikos, D. Poulikakos and R. Kroschewski, Biophysical journal, 2006, 90, 4380-4391.

Figure legends

Figure 1 – Schematic illustration of an LSFM and of the TC-LSFM perfusion chamber. **(a)** Principle of light sheet-based illumination microscope. A single plane in the specimen is laterally illuminated by a laser sheet. An objective lens placed at 90° with respect to the illumination axis (green arrow) collects the emitted fluorescence. By translating the specimen along the detection axis (red arrow), true optical sectioning is obtained. Since only the thin plane that is observed is illuminated, photobleaching and phototoxicity are minimized. **(b)** TC-LSFM perfusion chamber. The chamber features a heating plate at the bottom. A controller reading a sensor embedded in the chamber's body regulates its temperature. The temperature is maintained at a constant value of 37°C for mammalian cell culture. An inlet and an outlet for the medium perfusion are on the chamber's front wall. The specimen is illuminated with the laser light sheet through the side window. A water-dipping objective lens is plunged into the chamber and tightened by a spring-loaded O-ring. An autoclavable flexible Teflon foil connected to both the specimen holder and the chamber isolates the inside of the chamber and prevents contamination. The front window allows transmitted-light illumination of the specimen.

Figure 2 – Schematic illustration of the perfusion system used in the TC-LSFM. The red and yellow arrows indicate the flow direction of the cell culture media along the perfusion line. The inlet tubing, which provides the media supply, is composed of a gas-impermeable rubber tubing (red and yellow tubes) and a gas-permeable silicon tube. The 4 m long gas-permeable silicon spiral tubing is placed within a tight Plexiglas gas exchanger box containing the desired CO_2/air mixture (in our case 5% CO_2). The gas mixture is regulated by the CO_2 controller. The CO_2/air mixture diffuses through the silicon tube and saturates the flowing culture media. The gas-impermeable tubing outside the gas exchanger box prevents the contact of the medium with the laboratory atmosphere. The waste media outlet tubing (red tube in the picture at the top right) is connected to the outlet of the TC-LSFM-chamber. Both the media supply and the waste tubing are connected with a two-way precision peristaltic pump, which regulates the speed of the media flowing into and out of the TC-LSFM-chamber.

Figure 3 – TC-LSFM image contrast and resolution in the agarose container. **a**) A single MDCK cell aggregate embedded in collagen and inside an agarose container was imaged with the TC-LSFM in bright-field mode with an objective lens CZ Achroplan 40x/0.80 W Ph2. Inside the hollow cavity of the aggregate, the lumen, a small cluster of cells is visible (delimited by the dotted circle and marked by the arrowhead). **b**) The same MDCK aggregate

as in (**a**) is imaged with the TC-LSFM set-up (excitation lens CZ Plan-Neofluar 5x/0.16, detection lens CZ Achroplan 40x/0.80 W Ph2). Prior imaging, the cells were labeled with Syto61 (excitation line 633 nm, emission filter 680/60). Maximum projection of a raw TC-LSFM stack consisting of 29 slices at 1 µm spacing observed along six different directions. The three-dimensional morphology of the aggregate and the spatial arrangement of the small cell cluster inside the lumen (white arrowheads) are clearly visible. **c**) Individual slices along the z-axis from a three-dimensional image stack of the same aggregate as shown in (**a**) and (**b**) are shown. The corresponding depth in micrometers (Δz, starting from the first plane in the stack) is shown in each slice. The luminal cell cluster is clearly visible in several slices (e.g. Δz = 14 µm). **d, e**) Maximum projection of a 3D stack, rotated at 0° (**d**) and rotated by 45° (**e**). Each section has a thickness of 10 µm (projection of 10 slices at 1 µm spacing). Labeling: Syto61.

Figure 4 - Central plane images of stacks of a MDCK cyst recorded over time with the TC-LSFM. At each time point in the figure, a three-dimensional stack consisting of 50 slices spaced 0.5 µm was recorded. The fluorescence signals of middle planes (at a distance from the cyst bottom of ~ 25 µm) of GFP-actin are shown. The increase of the number of cells in the cyst, as well as that of the hollow lumen is detectable in the images of three consecutive days (excitation lens CZ Plan-Neofluar 5x/0.16, detection lens CZ Achroplan 40x/0.80 W Ph2, excitation line 488 nm, emission filter 488LP).

Figure 5 – The cell cycle length varies within individual lineage trees but not between experiments and over generations. (a) Each boxplot represents cell cycle lengths of individual cells within one lineage tree. The bottom and the top of the box are the first and third quartile. The line inside each box is the median (second quartile) cell cycle length. The cross refers to the outliers. The lineage trees 1 to 7 belong to experiment 1 (E1, grey background). The lineage trees 8 to 12 belong to experiment 2 (E2). While the median cell cycle length differs significantly among lineage trees ($p=0.0002$), it does not differ significantly between the experiments E1 and E2 ($p=0.1$). **(b)** Cell cycle length distributions over generation. No dependency of the cell cycle length on the number of generations is observed.

Figure 6 –A MDCK cell aggregate imaged for 84 hours. **(a)** The images show xy, xz, and yz average projections at different time points of a dividing MDCK cell labeled with H2B-YFP. The mitotic events are indicated by arrowheads. The smeared signal appearing at the time points t = 76h and t = 84h is a typical illumination artifact of the azimuthal (90°)

illumination in LSFM. Each cell focuses the laser light sheet similarly to a tiny lens. As the fluorescent signal diminishes over time and cell divisions (e.g. due to plasmid loss in the transient transfection) from t = 76h on, the intensity of the background fluorescence becomes closer to the signal and thus the autofluorescence of the medium appears as smear. This kind of artifacts can be reduced by reducing the autofluorescence of the surrounding medium, e.g. by employing phenol red-free or serum-free media. **(b)** The three-dimensional stacks were tracked in Imaris. The elapsed time is color-coded from 0 h to 84 h. The white squares represent the centroids of the MDCK cells recorded at t= 84 h (a). In order to provide an impression of the final shape of the aggregate, a cropped phase-contrast image of the aggregate is superimposed to the tracking. Scale bar 10 µm in both (a) and (b). **(c)** The development of the 11-cells clonal aggregate shown in (a) is represented by a cell lineage tree, G1 to G4 denote the different generation levels. Each node of the tree marks a cell division event. The branch lengths indicate complete, if the following mitosis is imaged, and incomplete cell cycle lengths of the individual cells. An identity number (e.g. cell 121) is assigned to each cell.

Figure 7 – The cell cycle lengths of two daughter cells can vary strongly. (a) The histogram shows the distribution of the difference in cell cycle lengths relative to the shortest cell cycle length of the two cells, in order to illustrate how different the cell cycle lengths of daughter cells can be. **(b)** The difference in cell cycle lengths of daughter cells at each generation (color-coded dots) in each lineage tree.

Figure 8 – Quantification of cell death over time. (**a**) Fragmented nuclei (arrowheads) indicate cell death events. The dotted lines highlight the contour of the aggregate at that specific time point. The contour was obtained from the transmitted light images. Scale bar 10 µm. (**b**) The cell death frequency does not systematically differ over the imaging time.

Figure 1

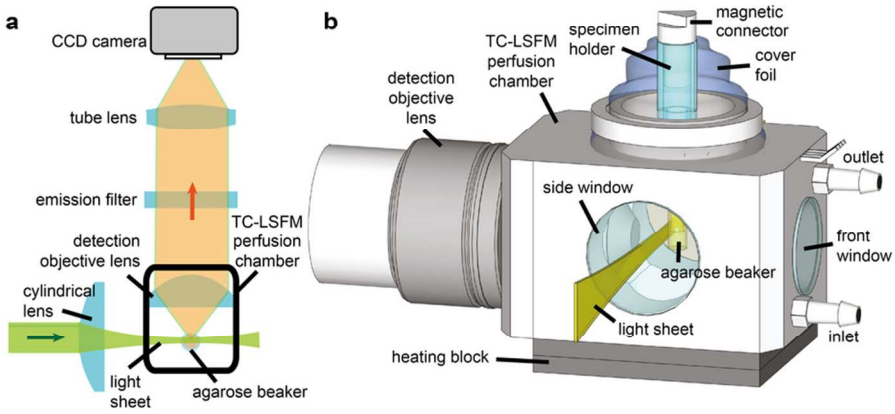

Figure 1 – Schematic illustration of an LSFM and of the TC-LSFM perfusion chamber. (a) Principle of light sheet-based illumination microscope. A single plane in the specimen is laterally illuminated by a laser sheet. An objective lens placed at 90° with respect to the illumination axis (green arrow) collects the emitted fluorescence. By translating the specimen along the detection axis (red arrow), true optical sectioning is obtained. Since only the thin plane that is observed is illuminated, photobleaching and phototoxicity are minimized. (b) TC-LSFM perfusion chamber. The chamber features a heating plate at the bottom. A controller reading a sensor embedded in the chamber's body regulates its temperature. The temperature is maintained at a constant value of 37°C for mammalian cell culture. An inlet and an outlet for the medium perfusion are on the chamber's front wall. The specimen is illuminated with the laser light sheet through the side window. A water-dipping objective lens is plunged into the chamber and tightened by a spring-loaded O-ring. An autoclavable flexible Teflon foil connected to both the specimen holder and the chamber isolates the inside of the chamber and prevents contamination. The front window allows transmitted-light illumination of the specimen.
88x45mm (300 x 300 DPI)

Figure 2

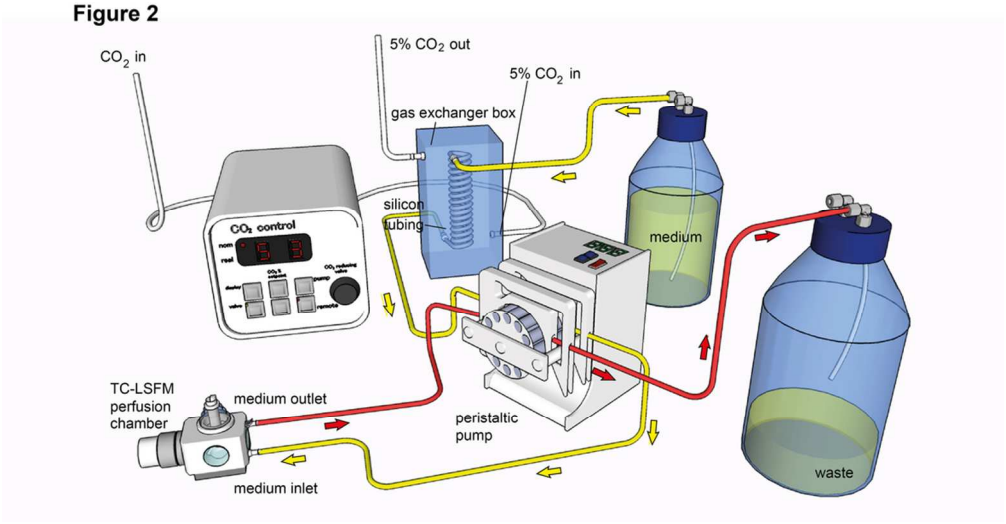

Figure 2 – Schematic illustration of the perfusion system used in the TC-LSFM. The red and yellow arrows indicate the flow direction of the cell culture media along the perfusion line. The inlet tubing, which provides the media supply, is composed of a gas-impermeable rubber tubing (red and yellow tubes) and a gas-permeable silicon tube. The 4 m long gas-permeable silicon spiral tubing is placed within a tight Plexiglas gas exchanger box containing the desired CO2/air mixture (in our case 5% CO2). The gas mixture is regulated by the CO2 controller. The CO2/air mixture diffuses through the silicon tube and saturates the flowing culture media. The gas-impermeable tubing outside the gas exchanger box prevents the contact of the medium with the laboratory atmosphere. The waste media outlet tubing (red tube in the picture at the top right) is connected to the outlet of the TC-LSFM-chamber. Both the media supply and the waste tubing are connected with a two-way precision peristaltic pump, which regulates the speed of the media flowing into and out of the TC-LSFM-chamber.
99x51mm (300 x 300 DPI)

Figure 3

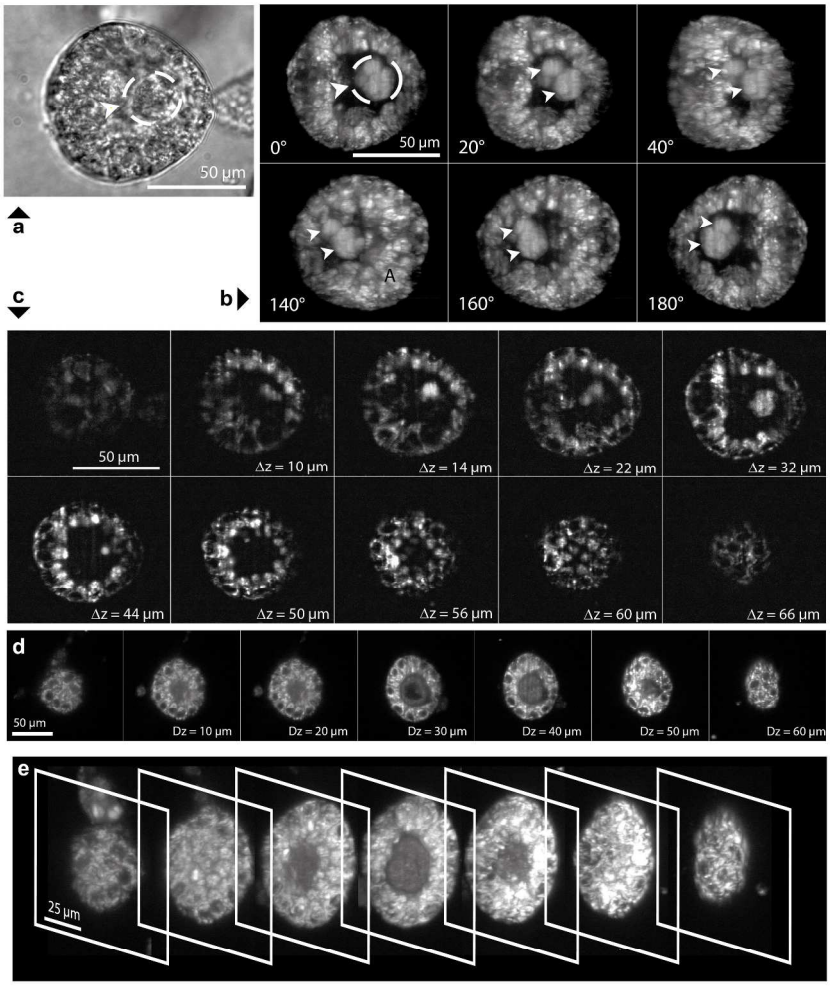

Figure 3 – TC-LSFM image contrast and resolution in the agarose container. a) A single MDCK cell aggregate embedded in collagen and inside an agarose container was imaged with the TC-LSFM in bright-field mode with an objective lens CZ Achroplan 40x/0.80 W Ph2. Inside the hollow cavity of the aggregate, the lumen, a small cluster of cells is visible (delimited by the dotted circle and marked by the arrowhead). b) The same MDCK aggregate as in (a) is imaged with the TC-LSFM set-up (excitation lens CZ Plan-Neofluar 5x/0.16, detection lens CZ Achroplan 40x/0.80 W Ph2). Prior imaging, the cells were labeled with Syto61 (excitation line 633 nm, emission filter 680/60). Maximum projection of a raw TC-LSFM stack consisting of 29 slices at 1 µm spacing observed along six different directions. The three-dimensional morphology of the aggregate and the spatial arrangement of the small cell cluster inside the lumen (white arrowheads) are clearly visible. c) Individual slices along the z-axis from a three-dimensional image stack of the same aggregate as shown in (a) and (b) are shown. The corresponding depth in micrometers (Δz, starting from the first plane in the stack) is shown in each slice. The luminal cell cluster is clearly visible in several slices (e.g. Δz = 14 µm). d, e) Maximum projection of a 3D stack, rotated at 0° (d) and rotated by

45° (e). Each section has a thickness of 10 µm (projection of 10 slices at 1 µm spacing). Labeling: Syto61.
233x317mm (300 x 300 DPI)

Figure 4

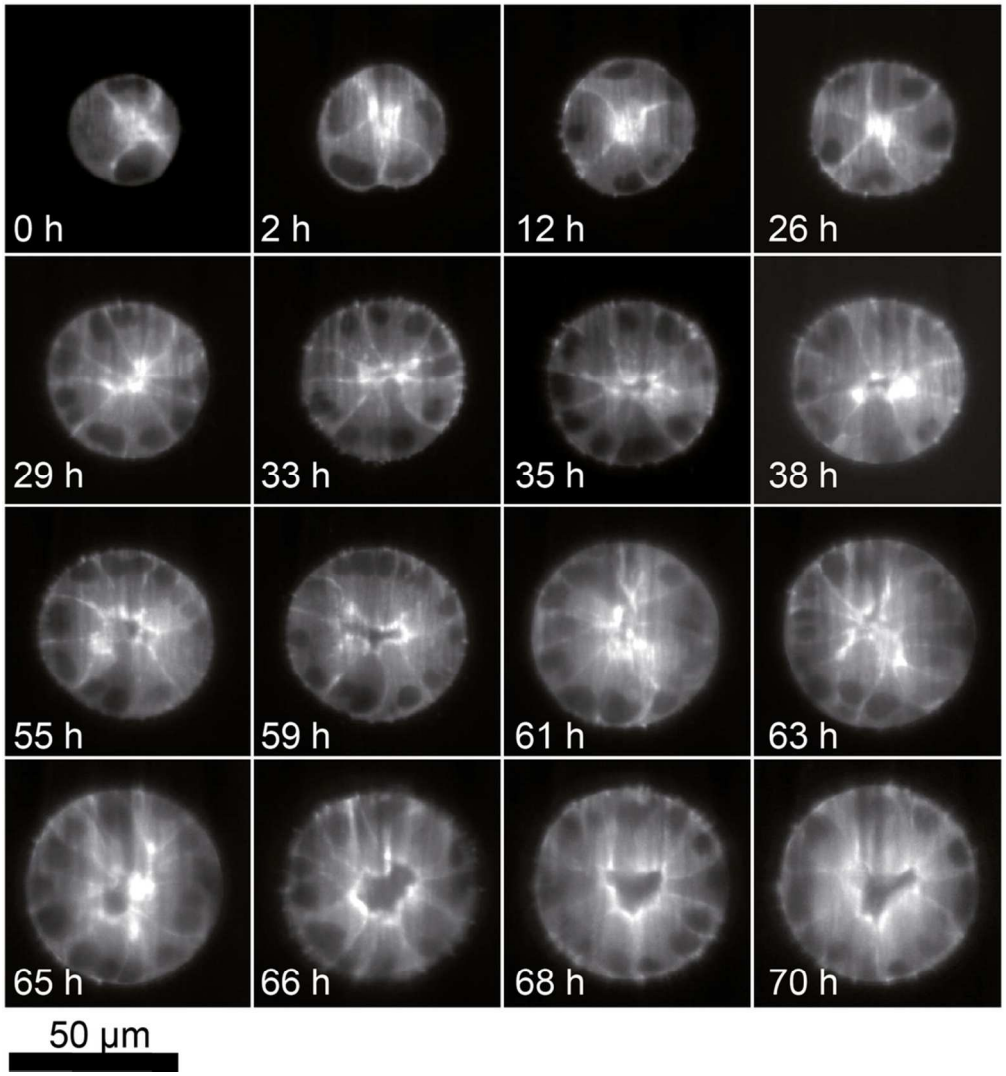

Figure 4 - Central plane images of stacks of a MDCK cyst recorded over time with the TC-LSFM. At each time point in the figure, a three-dimensional stack consisting of 50 slices spaced 0.5 µm was recorded. The fluorescence signals of middle planes (at a distance from the cyst bottom of ~ 25 µm) of GFP-actin are shown. The increase of the number of cells in the cyst, as well as that of the hollow lumen is detectable in the images of three consecutive days (excitation lens CZ Plan-Neofluar 5x/0.16, detection lens CZ Achroplan 40x/0.80 W Ph2, excitation line 488 nm, emission filter 488LP).
92x109mm (300 x 300 DPI)

Figure 5

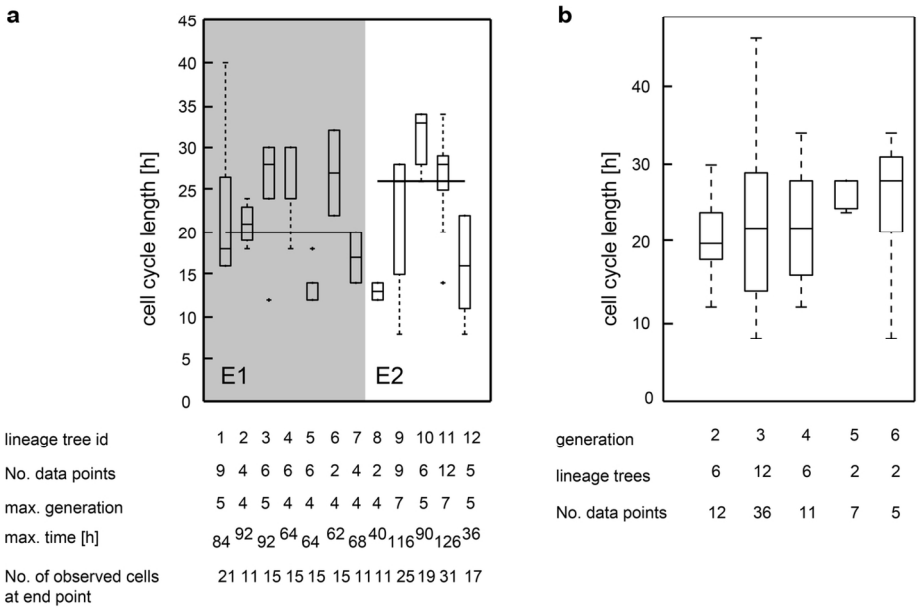

Figure 5 – The cell cycle length varies within individual lineage trees but not between experiments and over generations. (a) Each boxplot represents cell cycle lengths of individual cells within one lineage tree. The bottom and the top of the box are the first and third quartile. The line inside each box is the median (second quartile) cell cycle length. The cross refers to the outliers. The lineage trees 1 to 7 belong to experiment 1 (E1, grey background). The lineage trees 8 to 12 belong to experiment 2 (E2). While the median cell cycle length differs significantly among lineage trees ($p=0.0002$), it does not differ significantly between the experiments E1 and E2 ($p=0.1$). (b) Cell cycle length distributions over generation. No dependency of the cell cycle length on the number of generations is observed.
128x96mm (300 x 300 DPI)

Figure 6

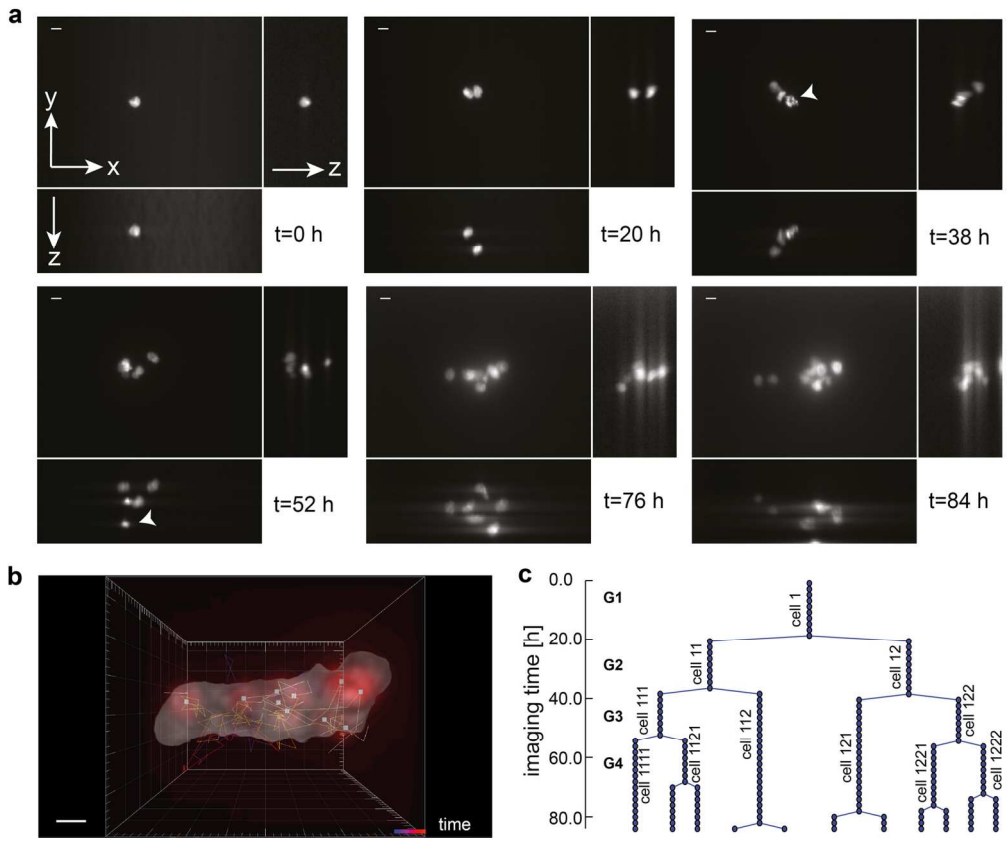

Figure 6 –A MDCK cell aggregate imaged for 84 hours. (a) The images show xy, xz, and yz average projections at different time points of a dividing MDCK cell labeled with H2B-YFP. The mitotic events are indicated by arrowheads. The smeared signal appearing at the time points t = 76h and t = 84h is a typical illumination artifact of the azimuthal (90°) illumination in LSFM. Each cell focuses the laser light sheet similarly to a tiny lens. As the fluorescent signal diminishes over time and cell divisions (e.g. due to plasmid loss in the transient transfection) from t = 76h on, the intensity of the background fluorescence becomes closer to the signal and thus the autofluorescence of the medium appears as smear. This kind of artifacts can be reduced by reducing the autofluorescence of the surrounding medium, e.g. by employing phenol red-free or serum-free media. (b) The three-dimensional stacks were tracked in Imaris. The elapsed time is color-coded from 0 h to 84 h. The white squares represent the centroids of the MDCK cells recorded at t= 84 h (a). In order to provide an impression of the final shape of the aggregate, a cropped phase-contrast image of the aggregate is superimposed to the tracking. Scale bar 10 µm in both (a) and (b). (c) The development of the 11-cells clonal aggregate shown in (a) is represented by a cell lineage tree, G1 to G4 denote the different generation levels. Each node of the tree marks a cell division event. The branch lengths indicate complete, if the following mitosis is imaged, and incomplete cell cycle lengths of the individual cells. An identity number (e.g. cell 121) is assigned to each cell.
145x128mm (300 x 300 DPI)

Figure 7

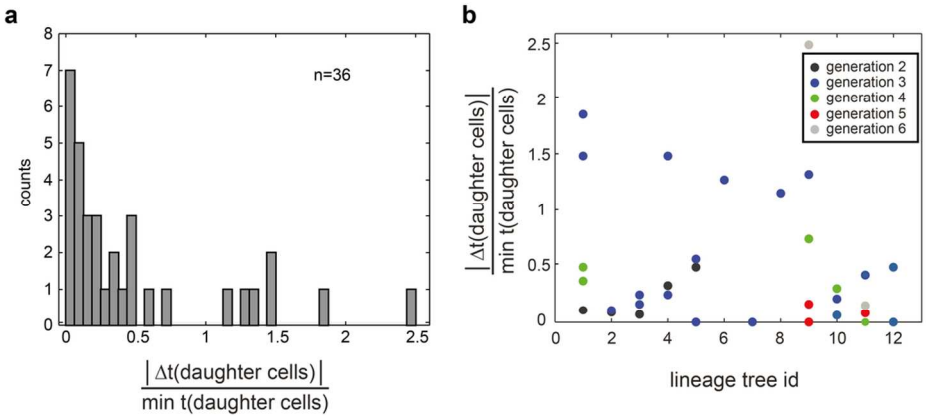

Figure 7 – The cell cycle lengths of two daughter cells can vary strongly. (a) The histogram shows the distribution of the difference in cell cycle lengths relative to the shortest cell cycle length of the two cells, in order to illustrate how different the cell cycle lengths of daughter cells can be. (b) The difference in cell cycle lengths of daughter cells at each generation (color-coded dots) in each lineage tree.
108x69mm (300 x 300 DPI)

Figure 8

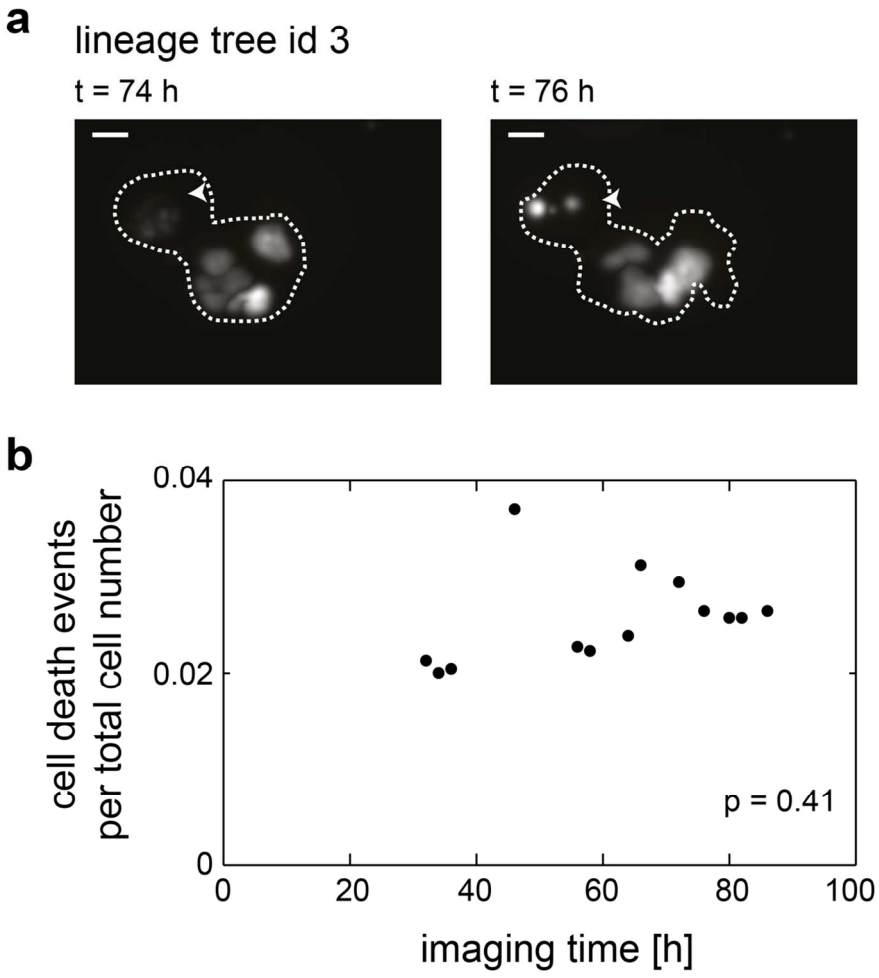

Figure 8 – Quantification of cell death over time. (a) Fragmented nuclei (arrowheads) indicate cell death events. The dotted lines highlight the contour of the aggregate at that specific time point. The contour was obtained from the transmitted light images. Scale bar 10 μm. (b) The cell death frequency does not systematically differ over the imaging time.
108x143mm (300 x 300 DPI)